Gas transfer velocities of CO_2 in subtropical monsoonal climate streams and small rivers

Siyue Li[a]*, Rong Mao[a], Yongmei Ma[a], Vedula V. S. S. Sarma[b]

a. Research Center for Eco-hydrology, Chongqing Institute of Green and Intelligent Technology, Chinese Academy of Sciences, Chongqing 400714, China

b. CSIR-National Institute of Oceanography, Regional Centre, Visakhapatnam, India

Correspondence

Siyue Li

Chongqing Institute of Green and Intelligent Technology (CIGIT),

Chinese Academy of Sciences (CAS).

266, Fangzheng Avenue, Shuitu High-tech Park, Beibei, Chongqing 400714, China.

Tel: +86 23 65935058; Fax: +86 23 65935000

Email: syli2006@163.com

Abstract

CO_2 outgassing from rivers is a critical component for evaluating riverine carbon cycle, but it is poorly quantified largely due to limited measurements and modeling of gas transfer velocity in subtropical streams and rivers. We measured CO_2 flux rates, and calculated k and partial pressure (pCO_2) in 60 river networks of the Three Gorges Reservoir (TGR) region, a typical area in the upper Yangtze River with monsoonal climate and mountainous terrain. The determined k_{600} (gas transfer velocity normalized to a Schmidt number of 600 (k_{600}) at a temperature of 20 ℃) value (48.4±53.2 cm/h) showed large variability due to spatial variations in physical processes on surface water turbulence. Our flux-derived k values using chambers were comparable with model derived from flow velocities based on a subset of data. Unlike in open waters, e.g. lakes, k_{600} is more pertinent to flow velocity and water depth in the studied river systems. Our results show that TGR river networks emitted approx. 0.69 to 0.71 Tg CO_2 (1 Tg=10^{12} g) during monsoon period using varying approaches such as chambers, derived k_{600} values and model. This study suggests that incorporating scale-appropriate k measurements into extensive pCO_2 investigations are required to refine basin-wide carbon budgets in the subtropical streams and small rivers. We concluded that simple parameterization of k_{600} as a function of morphological characteristics is site specific for regions / watersheds and hence highly variable in rivers of the upper Yangtze. K_{600} models should be developed for stream studies to evaluate the contribution of these regions to the atmospheric CO_2.

Key words: CO_2 outgassing, riverine C flux, flow velocity, physical controls, Three

Gorge Reservoir, Yangtze River

1. Introduction

Rivers serve as a significant contributor of CO_2 to the atmosphere (Raymond et al., 2013;Cole et al., 2007;Li et al., 2012;Tranvik et al., 2009). As a consequence, accurate quantification of riverine CO_2 emissions is a key component to estimate net continental carbon (C) flux (Raymond et al., 2013). More detailed observational data and accurate measurement techniques are critical to refine the riverine C budgets (Li and Bush, 2015;Raymond and Cole, 2001). Generally two methods are used to estimate CO_2 areal fluxes from the river system, such as direct measurements using floating chambers (FCs), and indirect calculation of thin boundary layer (TBL) model, which is depended on gas concentration gradient at air-water interface and gas transfer velocity, k (Guerin et al., 2007;Xiao et al., 2014). Direct measurements are normally laborious, while the latter method is ease and simple and thus is preferred (Butman and Raymond, 2011;Lauerwald et al., 2015;Li et al., 2013;Li et al., 2012;Ran et al., 2015).

The areal flux of CO_2 (F, mmol/m^2/d) *via* the water–air interface by TBL is described as follows:

$$F = k \times K_h \times \triangle pCO_2 \qquad (1)$$

$$K_h = 10^{-(1.11 + 0.016 * T - 0.00007 * T^2)} \qquad (2)$$

where k (m/d) is the gas transfer velocity of CO_2 (also referred to as piston velocity) at the *in situ* temperature (Li et al., 2016). $\triangle pCO_2$ (μatm) is the pCO_2 gradient at air-water interface (Borges et al., 2004). K_h (mmol/m^3/μatm) is the aqueous-phase solubility coefficient of CO_2 corrected using *in situ* temperature (T in ℃) (Li et al., 2016).

△pCO_2 can be measured well in various aquatic systems, however, the accuracy of the estimation of flux is depended on the k value. Broad ranges of k for CO_2 (Raymond and Cole, 2001;Raymond et al., 2012;Borges et al., 2004) were reported due to variations in techniques, tracers used and governing processes. k is controlled by turbulence at the surface aqueous boundary layer, hence, k_{600} (the standardized gas transfer velocity at a temperature of 20 ^{0}C is valid for freshwater) is parameterized as a function of wind speed in open water systems of reservoirs, lakes, and oceans (Borges et al., 2004;Guerin et al., 2007;Wanninkhof et al., 2009). While in streams and small rivers, turbulence at the water-air interface is generated by shear stresses at streambed, thus k is modeled using channel slope, water depth, and water velocity in particular (Raymond et al., 2012;Alin et al., 2011). Variable formulations of k have been established by numerous theoretical, laboratory and field studies, nonetheless, better constraint on k levels is still required as its levels are very significant and specific due to large heterogeneity in hydrodynamics and physical characteristics of river networks. This highlights the importance of k measurements in a wide range of environments for accurate upscaling of CO_2 evasion, and for parameterizing the physical controls on k_{600}. However, only few studies provide information of k for riverine CO_2 flux in Asia (Alin et al., 2011;Ran et al., 2015), and those studies do not address the variability of k in China's small rivers and streams.

Limited studies demonstrated that higher levels of k in the Chinese large rivers (Liu et al., 2017;Ran et al., 2017;Ran et al., 2015;Alin et al., 2011), which contributed to much higher CO_2 areal flux particularly in China's monsoonal rivers that are impacted by hydrological seasonality. The monsoonal flow pattern and thus flow velocity is expected to be different than other rivers in the world, as a consequence, k levels should be different than others, and potentially is higher in subtropical monsoonal rivers.

Considerable efforts, such as purposeful (Crusius and Wanninkhof, 2003;Jean-Baptiste and Poisson, 2000) and natural tracers (Wanninkhof, 1992) and FCs (Alin et al., 2011;Borges et al., 2004;Prytherch et al., 2017;Guerin et al., 2007), have been carried out to estimate accurate k values. The direct determination of k by FCs is more popular due to simplicity of the technique for short-term CO_2 flux measurements (Prytherch et al., 2017;Raymond and Cole, 2001;Xiao et al., 2014). Prior reports, however, have demonstrated that k values and the parameterization of k as a function of wind and/or flow velocity (probably water depth) vary widely across rivers and streams (Raymond and Cole, 2001;Raymond et al., 2012). To contribute to this debate, extensive investigation was firstly accomplished for determination of k in rivers and streams of the upper Yangtze using FC method. Models of k were further developed using hydraulic properties (i.e., flow velocity, water depth) by flux measurements with chambers and TBL model. Our recent study preliminarily investigated pCO_2 and air – water CO_2 areal flux as well as their controls from fluvial networks in the Three Gorges Reservoir (TGR) area (Li et al., 2018). The past study was based on two field works, and the diffusive models from other rivers / regions were used. Here, we derive k levels and develop the gas transfer model in this area (mountainous streams and small rivers) for more accurate quantification of CO_2 areal flux, and also to serve for the fluvial networks in the Yangtze River or others with similar hydrology and geomorphology. Moreover, we did detail field campaigns in the two contrasting rivers: Daning and Qijiang for models (Fig. 1), the rest were TGR streams and small rivers (abbreviation in TGR rivers). The study thus clearly stated distinct differences than the previous study (Li et al., 2018) by the new contributions of specific objectives and data supplements, as well as wider significance. Our new contributions to the literature thus include (1) determination and controls of k levels for small rivers and streams in subtropical areas of China, and (2) new models developed in the subtropical mountainous river networks. The outcome of this study is expected to help in accurate estimation of CO_2 evasion from subtropical rivers and streams, and thus refine riverine C budget over a regional/basin scale.

2. Materials and methods

2.1. Study areas

All field measurements were carried out in the rivers and streams of the Three Gorges Reservoir (TGR) region (28°44′–31°40′N, 106°10′–111°10′E) that is locating in the upper Yangtze River, China (Fig. 1). This region is subject to humid subtropical monsoon climate with an average annual temperature ranging between15 and 19 ℃. Average annual precipitation is approx. 1250 mm with large intra- and inter-annual variability. About 75% of the annual total rainfall is concentrated between April and September (Li et al., 2018).

The river sub-catchments include large scale river networks covering the majority of the tributaries of the Yangtze in the TGR region, i.e., data of 48 tributaries were collected. These tributaries have drainage areas that vary widely from 100 to 4400 km^2 with width ranging from 1 m to less than 100 m. The annual discharges from these tributaries have a broad spectrum of 1.8 – 112 m^3/s. Detailed samplings were conducted in the two largest rivers of Daning (35 sampling sites) and Qijiang (32 sites) in the TGR region. These two river basins drain catchment areas of 4200 and 4400 km^2.The studied river systems had width < 100 m, we thus defined them as small rivers and streams. The Daning and Qijiang river systems are underlain by widely carbonate rock, and locating in a typical karst area. The location of sampling sites is deciphered in Fig. 1. The detailed information on sampling sites and primary data are presented in the Supplement Materials (Appendix Table A1). The sampling sites are outside the Reservoirs and are not affected by dam operation.

2.2. Water sampling and analyses

Three fieldwork campaigns from the main river networks in the TGR region were undertaken during May through August in 2016 (i.e., 18-22 May for Daning, 21 June-2 July for the entire tributaries of TGR, and 15-18 August for Qijiang). A total of 115 discrete grab samples were collected (each sample consisted of three replicates). Running waters were taken using pre acid-washed 5-L high density polyethylene (HDPE) plastic containers from depths of 10 cm below surface. The samples were filtered through pre-baked Whatman GF/F (0.7-µm pore size) filters on the sampling day and immediately stored in acid-washed HDPE bottles. The bottles were transported in ice box to the laboratory and stored at 4 ℃ for analysis. Concentrations of dissolved organic carbon (DOC) were determined within 7 days of water collection (Mao et al., 2017).

Water temperature (T), *p*H, DO saturation (DO%) and electrical conductivity (EC) were measured *in situ* by the calibrated multi-parameter sondes (HQ40d HACH, USA, and YSI 6600, YSI incorporated, USA). pH, the key parameter for pCO_2 calculation, was measured to a precision of ± 0.01, and pH sonde was calibrated by the certified reference materials (CRMs) before measurements with an accuracy of better than $\pm 0.2\%$. Atmospheric CO_2 concentrations were determined *in situ* using EGM-4 (Environmental Gas Monitor; PP SYSTEMS Corporation, USA). Total alkalinity was measured using a fixed endpoint titration method with 0.0200 mol/L hydrochloric acid (HCl) on the sampling day. DOC concentration was measured using a total organic carbon analyzer (TOC-5000, Shimadzu, Japan) with a precision better than 3% (Mao et al., 2017). All the used solvents and reagents in experiments were of analytical-reagent grade.

Concomitant stream width, depth and flow velocity were determined along the cross section, and flow velocity was determined using a portable flow meter LS300-A (China), the meter shows an error of <1.5%. Wind speed at 1 m over the water surface (U_1) and air temperature (Ta) were measured with a Testo 410-1 handheld anemometer (Germany). Wind speed at 10 m height (U_{10}, unit in m/s) was calculated using the following formula (Crusius and Wanninkhof, 2003):

$$U_{10} = U_Z\left[1+\frac{(C_{d10})^{1/2}}{K}\times \ln\left(\frac{10}{z}\right)\right] \quad (3)$$

where C_{d10} is the drag coefficient at 10 m height (0.0013 m/s), and K is the von Karman constant (0.41), and z is the height (m) of wind speed measurement. U_{10}=1.208×U_1 as we measured the wind speed at a height of 1m (U_1).

Aqueous pCO_2 was computed from the measurements of pH, total alkalinity, and water temperature using CO_2 System (k_1 and k_2 are from Millero, 1979) (Lewis et al., 1998). This program can yield high quality data (Li et al., 2013;Li et al., 2012;Borges et al., 2004).

2.3. Water-to-air CO_2 fluxes using FC method

FCs (30 cm in diameter, 30 cm in height) were deployed to measure air-water CO_2 fluxes and transfer velocities. They were made of cylindrical polyvinyl chloride (PVC) pipe with a volume of 21.20 L and a surface area of 0.071 m^2. These non-transparent, thermally insulated vertical tubes, covered by aluminum foil, were connected *via* CO_2 impermeable rubber-polymer tubing (with outer and inner diameters of 0.5 cm and 0.35 cm, respectively) to a portable non-dispersive infrared CO_2 analyzer EGM-4 (PPSystems). Air was circulated through the EGM-4 instrument *via* an air filter using an integral pump at a flow rate of 350 ml/min. The chamber method was widely used and more details of advantages and limits on chambers were reviewed elsewhere (Alin et al., 2011;Borges et al., 2004;Xiao et al., 2014).

Chamber measurements were conducted by deploying two replicate chambers or one chamber for two times at each site. In sampling sites with low and favorable flow conditions (Fig. S1), freely drifting chambers (DCs) were executed, while sampling sites in rivers and streams with higher flow velocity were conducted with anchored chambers (ACs) (Ran et al., 2017). DCs were used in sampling sites with current velocity of < 0.1 m/s, this resulted in limited sites (a total of 6 sites) using DCs. ACs would create overestimation of CO_2 emissions by a factor of several folds (i.e., > 2) in our study region (Lorke et al., 2015). Data were logged automatically and continuously at 1-min interval over a given span of time (normally 5-10 minutes) after enclosure. The CO_2 area flux ($mg/m^2/h$) was calculated using the following formula.

$$F = 60 \times \frac{dpco2 \times M \times P \times T_0}{dt \times V_0 \times P_0 \times T} H \qquad (4)$$

Where $dpco_2/dt$ is the rate of concentration change in FCs (μl/l/min); M is the molar mass of CO_2 (g/mol); P is the atmosphere pressure of the sampling site (Pa); T is the chamber absolute temperature of the sampling time (K); V_0 is the molar volume (22.4 l/mol), P_0 is atmosphere pressure (101325 Pa), and T_0 is absolute temperature (273.15 K) under the standard condition; H is the chamber height above the water surface (m) (Alin et al., 2011). We accepted the flux data that had a good linear regression of flux against time ($R^2 \geq 0.95$, $p<0.01$) following manufacturer' specification. In our sampling points, all measured fluxes were retained since the floating chambers yielded linearly increasing CO_2 against time.

Water samples from a total of 115 sites were collected. Floating chambers with replicates were deployed in 101 sites (32 sampling sites in Daning, 37 sites in TGR river networks and 32 sites in Qijiang). The sampling period covered spring and summer season, our sampling points are reasonable considering a water area of 433 km^2. For example, 16 sites were collected for Yangtze system to examine hydrological and geomorphological controls on pCO_2 (Liu et al., 2017), and 17 sites for dynamic biogeochemical controls on riverine pCO_2 in the Yangtze basin (Liu et al., 2016). Similar to other studies, sampling and flux measurements in the day would tend to underestimate CO_2 evasion rate (Bodmer et al., 2016).

2.4. Calculations of the gas transfer velocity

The k was calculated by reorganizing Eq (1). To make comparisons, k is normalized to a Schmidt (Sc) number of 600 (k_{600}) at a temperature of 20 ℃.

$$k_{600} = k_T\left(\frac{600}{S_{CT}}\right)^{-0.5} \qquad (5)$$

$$S_{CT} = 1911.1 - 118.11T + 3.4527T^2 - 0.04132T^3 \qquad (5)$$

Where k_T is the measured values at the *in situ* temperature (T, unit in ^{o}C), S_{CT} is the Schmidt number of temperature T. Dependency of -0.5 was employed here as measurement were made in turbulent rivers and streams in this study (Alin et al., 2011;Borges et al., 2004;Wanninkhof, 1992).

2.5. Estimation of river water area

Water surface is an important parameter for CO_2 efflux estimation, while it depends on its climate, channel geometry and topography. River water area therefore largely fluctuates with much higher areal extent of water surface particularly in monsoonal season. However, most studies do not consider this change, and a fraction of the drainage area is used in river water area calculation (Zhang et al., 2017). In our study, a 90 m resolution SRTM DEM (Shuttle Radar Topography Mission digital elevation model) data and Landsat images in dry season were used to delineate river network, and thus water area (Zhang et al., 2018), whilst, stream orders were not extracted. Water area of river systems is generally much higher in monsoonal season in comparison to dry season, for instance, Yellow River showed 1.4-fold higher water area in the wet season than in the dry season (Ran et al., 2015). Available dry-season image was likely to underestimate CO_2 estimation.

2.6. Data processing

Prior to statistical analysis, we excluded k_{600} data for samples with the air-water pCO_2 gradient <110 μatm, since the error in the k_{600} calculations drastically enhances when $\triangle pCO_2$ approaches zero (Borges et al., 2004;Alin et al., 2011), and datasets with $\triangle pCO_2$ >110 μatm provide an error of <10% on k_{600} computation. Thus, we discarded the samples (36.7% of sampling points with flux measurements) with $\triangle pCO_2$ <110 μatm for k_{600} model development, while all samples were included for the flux estimations from diffusive TBL model and floating chambers.

Spatial differences (Daning, Qijiang and entire tributaries of TGR region) were tested using the nonparametric Mann Whitney U-test. Multivariate statistics, such as correlation and stepwise multiple linear regression, were performed for the models of k_{600} using potential physical parameters of wind speed, water depth, and current velocity as the independent variables (Alin et al., 2011). Data analyses were conducted from both separated data and combined data of river systems. k models were obtained by water depth using data from the TGR rivers, while by flow velocity in the Qijiang, whilst, models were not developed for Daning and combined data. All statistical relationships were significant at $p < 0.05$. The statistical processes were conducted using SigmaPlot 11.0 and SPSS 16.0 for Windows (Li et al., 2009;Li et al., 2016).

3. Results

3.1. CO_2 partial pressure and key water quality variables

Significant spatial variations in water temperature, pH, pCO_2 and DOC were observed among Daning, TGR and Qijiang rivers whereas alkalinity did not display such variability (Fig. S2). *p*H varied from 7.47 to 8.76 with exceptions of two quite high values of 9.38 and 8.87 (total mean: 8.39 ± 0.29). Significantly lower *p*H was observed in TGR rivers (8.21 ± 0.33) (Table 1; $p<0.001$; Fig. S2). pCO_2 varied between 50 and 4830 μatm with mean of 846 ± 819 μatm (Table 1). There were 28.7% of samples that had pCO_2 levels lower than 410 μatm, while the studied rivers were overall supersaturated with reference to the atmospheric CO_2 and act as a source for the atmospheric CO_2. The pCO_2 levels were 2.1 to 2.6-fold higher in TGR rivers than Daning (483 ± 294 μatm) and Qijiang Rivers (614 ± 316 μatm) (Fig. S2).

There was significantly higher concentration of DOC in the TGR rivers (12.83 ± 7.16 mg/l) than Daning and Qijiang Rivers (3.76 ± 5.79 vs 1.07 ± 0.33 mg/l in Qijiang and Daning) ($p<0.001$; Fig. S3). Moreover, Qijiang showed significantly higher concentration of DOC than Daning (3.76 ± 5.79 vs 1.07 ± 0.33 mg/l in Qijiang and Daning) ($p<0.001$ by Mann-Whitney Rank Sum Test; Fig. S3).

3.2. CO_2 flux using floating chambers

The calculated CO_2 areal fluxes were higher in TGR rivers (217.7 ± 334.7 mmol/m^2/d, n = 35), followed by Daning (122.0 ± 239.4 mmol/m^2/d, n = 28) and Qijiang rivers (50.3 ± 177.2 mmol/m^2/d, n = 32) (Fig. 2). The higher CO_2 evasion from the TGR rivers is consistent with high riverine pCO_2 levels. The mean CO_2 emission rate was 133.1 ± 269.1 mmol/m^2/d (n = 95) in all three rivers sampled. The mean CO_2 flux differed significantly between TGR rivers and Qijiang (Fig. 2).

3.3. k levels

A total of 64 data were used (10 for Daning River, 33 for TGR rivers and 21 for Qijiang River) to develop k model after removal of samples with $\triangle pCO_2$ less than 110 μatm (Table 2). No significant variability in k_{600} values were observed among the three rivers sampled (Fig. 3). The mean k_{600} was relatively higher in Qijiang (60.2 ± 78.9 cm/h), followed by Daning (50.2 ± 20.1 cm/h) and TGR rivers (40.4 ± 37.6 cm/h), while the median k_{600} was higher in Daning (50.5cm/h), followed by TGR rivers (30.0 cm/h) and Qijiang (25.8 cm/h) (Fig. 3; Table S1). Combined k_{600} data were averaged to 48.4 ± 53.2 cm/h (95% CI: 35.1-61.7), and it is 1.5-fold higher than the median value (32.2 cm/h) (Fig. 3).

Contrary to our expectations, no significant relationship was observed between k_{600} and water depth, and current velocity using the entire data in the three river systems (TGR streams and small rivers, Danning and Qjiang) (Fig. S4). There were not statistically significant relationships between k_{600} and wind speed using separated data or combined data. Flow velocity showed slightly linear relation with k_{600}, and the extremely high value of k_{600} was observed during the periods of higher flow velocity (Fig. S4a) using combined data. Similar trend was also observed between water depth and k_{600} values (Fig. S4b). k_{600} as a function of water depth was obtained in the TGR rivers, but it explained only 30% of the variance in k_{600}. However, model using data from Qijiang could explain 68% of the variance in k_{600} (Fig. 4b), and it was in line with general theory.

4. Discussion

4.1. Uncertainty assessment of pCO_2 and flux-derived k_{600} values

The uncertainty of flux-derived k values mainly stem from ΔpCO_2 and flux measurements (Bodmer et al., 2016;Golub et al., 2017;Lorke et al., 2015). Thus we provided uncertainty assessments caused by dominant sources of uncertainty from measurements of aquatic pCO_2 and CO_2 areal flux since uncertainty of atmospheric CO_2 measurement could be neglected.

In our study, aquatic pCO_2 was computed based on pH, alkalinity and water temperature rather than directly measured. Recent studies highlighted pCO_2 uncertainty caused by systematic errors over empiric random errors (Golub et al., 2017). Systematic errors are mainly attributed to instrument limitations, i.e., sondes of pH and water temperature. The relative accuracy of temperature meters was $\pm 0.1\ ^0C$

according to manufacturers' specifications, thus the uncertainty of water T propagated on uncertainty in pCO_2 was minor (Golub et al., 2017). Systematic errors therefore stem from pH, which has been proved to be a key parameter for biased pCO_2 estimation calculated from aquatic carbon system (Li et al., 2013;Abril et al., 2015). We used a high accuracy of pH electrode and the pH meters were carefully calibrated using CRMs, and *in situ* measurements showed an uncertainty of ±0.01. We then run an uncertainty of ±0.01 pH to quantify the pCO_2 uncertainty, and an uncertainty of ±3% was observed. Systematic errors thus seemed to show little effects on pCO_2 errors in our study.

Random errors are from repeatability of carbonate measurements. Two replicates for each sample showed the uncertainty of within ±5%, indicating that uncertainty in pCO_2 calculation from alkalinity measurements could be minor.

The measured pH ranges also exhibited great effects on pCO_2 uncertainty (Hunt et al., 2011;Abril et al., 2015). At low pH, pCO_2 can be overestimated when calculated from pH and alkalinity (Abril et al., 2015). Samples for CO_2 fluxes estimated from pH and alkalinity showed pH average of 8.39±0.29 (median 8.46 with quartiles of 8.24-8.56) (n=115). Thus, overestimation of calculated CO_2 areal flux from pH and alkalinity is likely to be minor. Further, contribution of organic matter to non-carbonate alkalinity is likely to be neglected because of low DOC (mean 6.67 mg/L; median 2.51 mg/L) (Hunt et al., 2011;Li et al., 2013).

Efforts have been devoted to measurement techniques (comparison of FC, eddy covariance-EC and boundary layer model-BLM) for improving CO_2 quantification from rivers because of a notable contribution of inland waters to the global C budget, which could have a large effect on the magnitude of the terrestrial C sink. Whilst, prior studies reported inconsistent trends of CO_2 area flux by these methods. For instance, CO_2 areal flux from FC was much lower than EC (Podgrajsek et al., 2014), while areal flux from FC was higher than both EC and BLM elsewhere (Erkkila et al., 2018), however, Schilder et al (Schilder et al., 2013) demonstrated that areal flux from BLM was 33-320% of *in-situ* FC measurements. Albeit unsatisfied errors of varied techniques and additional perturbations from FC occurs, however, FC method is currently a simple and preferred technique for CO_2 flux because that choosing a right k value remains a major challenge and others require high workloads (Martinsen et al., 2018).

Recent study further reported fundamental differences in CO_2 emission rates between ACs and freely DFs (Lorke et al., 2015), i.e., ACs biased the gas areal flux higher by a factor of 2.0-5.5. However, some studies observed that ACs showed reasonable agreement with other flux measurement techniques (Galfalk et al., 2013), and this method is straightforward, inexpensive and relatively simple hence it is widely used (Ran et al., 2017). Water-air interface CO_2 flux measurements were primarily made using ACs in our studied streams and small rivers because of relatively high current velocity; otherwise, floating chambers will travel far during the measurement period. In addition, inflatable rings were used for sealing the chamber headspace and submergence of ACs was minimal, therefore, our measurements were potentially overestimated, but reasonable. We could not test the overestimation of ACs in this study, the modified FCs, i.e., DCs and integration of ACs and DCs, and multi-method comparison study including FCs, ECs and BLM should be conducted for a reliable chamber method.

Our model was from a subset of the data (i.e., Qijiang), while CO_2 flux from our model was in good agreement with the fluxes from FC, determined k and other models when the developed model was applied for the whole dataset (please refer to Tables 2 and 3). The comparison of the fluxes from variable methods suggested that the model can be used for riverine CO_2 flux at catchment scale or regional scale though it cannot be used at individual site. Recent studies, however, did not test the applicability of models when k_{600} models from other regions were employed. Our k_{600} values were close to the average of Ran et al. (2015) (measured with drifting chambers) and Liu et al. (2017) (measured with static chambers in canoe shape), this indicated that our potential overestimation was limited. However, since we had very limited drifting chamber measurements because of high current velocity, the relationships with chamber derived k_{600} values and flow velocity/depth only with the drifting chamber data could not be tested. Whereas, we acknowledged that k_{600} could be over-estimated using AFs.

The extremely high values (two values of 260 and 274 cm/h) are outside of the global ranges and also considerably higher than k_{600} values in Asian rivers. Furthermore, the revised model was comparable to the published models (Fig. 4), i.e., models of Ran et al. (2015) (measured with drifting chambers) and Liu et al. (2017) (measured with static chambers in canoe shape), which suggested that exclusion of the two extremely values were reasonable, and this was further supported by the CO_2 flux using different approaches (Tables 2 and 3).

Sampling seasonality considerably regulated riverine pCO_2 and gas transfer velocity and thus water-air interface CO_2 evasion rate (Ran et al., 2015;Li et al., 2012). We sampled waters in wet season (monsoonal period) due to that it showed wider range of flow velocity and thus it covered the k_{600} levels in the whole hydrological season. Wet season generally had higher current velocity and thus higher gas transfer velocity (Ran et al., 2015), while aquatic pCO_2 was variable with seasonality. We recently reported that riverine pCO_2 in the wet season was 81% the level in the dry season (Li et al., 2018), and prior study on the Yellow River reported that k level in the wet season was 1.8-fold higher than in the dry season (Ran et al., 2015), while another study on the Wuding River demonstrated that k level in the wet season was 83%-130% of that in the dry season (Ran et al., 2017). Thus, we acknowledged a certain amount of errors on the annual flux estimation from sampling campaigns during the wet season in the TGR area, while this uncertainty could not be significant because that the diluted pCO_2 could alleviate the overestimated emission by increased k level in the wet season (stronger discussion please refer to SOM).

4.2. Determined k values relative to world rivers

We derived first-time the k values in the subtropical streams and small rivers. Our determined k_{600} levels with a 95% CI of 35.1 to 61.7 (mean: 48.4) cm/h is compared well with a compilation of data for streams and small rivers (e.g., 3-70 cm/h) (Raymond et al., 2012). Our determined k_{600} values are greater than the global rivers' average (8 - 33 cm/h) (Raymond et al., 2013;Butman and Raymond, 2011), and much higher than mean for tropical and temperate large rivers (5-31 cm/h) (Alin et al., 2011). These studies evidences that k_{600} values are highly variable in streams and small rivers (Alin et al., 2011;Ran et al., 2015). Though the mean k_{600} in the TGR, Daning and Qijiang is higher than global mean, however, it is consistent with k_{600} values in the main stream and river networks of the turbulent Yellow River (42 ± 17 cm/h) (Ran et al., 2015), and Yangtze (38 ± 40 cm/h) (Liu et al., 2017) (Table S2).

The calculated pCO_2 levels were within the published range, but towards the lower-end of published concentrations compiled elsewhere (Cole and Caraco, 2001;Li et al., 2013). The total mean pCO_2 (846 ± 819 μatm) in the TGR, Danning and Qijiang rivers was one third lower than global river's average (3220 μatm) (Cole and Caraco, 2001). The lower pCO_2 than most of the world's river systems, particularly the under-saturated values, demonstrated that heterotrophic respiration of terrestrially derived DOC was not significant. Compared with high alkalinity, the limited delivery of DOC particularly in the Daning and Qijiang river systems (Figs. S2 and S3) also indicated that in-stream respiration was limited. These two river systems are characterized by karst terrain and underlain by carbonate rock, where photosynthetic uptake of dissolved CO_2 and carbonate minerals dissolution considerably regulated aquatic pCO_2 (Zhang et al., 2017).

Higher pH levels were observed in Daning and Qijiang river systems ($p<0.05$ by Mann-Whitney Rank Sum Test), where more carbonate rock exists that are characterized by karst terrain. Our pH range was comparable to the recent study on the karst river in China (Zhang et al., 2017). Quite high values (8.39 ±0.29, ranging between 7.47 and 9.38; 95% confidence interval: 8.33-8.44) could increase the importance of the chemical enhancement, nonetheless, few studies did take chemical enhancement into account (Wanninkhof and Knox, 1996;Alshboul and Lorke, 2015). The chemical enhancement can increase the CO_2 areal flux by a factor of several folds in lentic systems with low gas transfer velocity, whist enhancement factor decreased quickly as k_{600} increased (Alshboul and Lorke, 2015). Our studied rivers are located in mountainous area with high k_{600}, which could cause minor chemical enhancement factor. This chemical enhancement of CO_2 flux was also reported to be limited in high-pH and also turbulent rivers (Zhang et al., 2017).

4.3. Hydraulic controls of k_{600}

It has been well established that k_{600} is governed by a multitude of physical factors particularly current velocity, wind speed, stream slope and water depth, of which, wind speed is the dominant factor of k in open waters such as large rivers and estuaries (Alin et al., 2011;Borges et al., 2004;Crusius and Wanninkhof, 2003;Raymond and Cole, 2001). In contrast k_{600} in small rivers and streams is closely linked to flow velocity, water depth and channel slope (Alin et al., 2011;Raymond et al., 2012). Several studies reported that the combined contribution of flow velocity and wind speed to k is significant in the large rivers (Beaulieu et al., 2012;Ran et al., 2015). Thus, k_{600} values are higher in the Yellow River (ca. 0-120 cm/h) as compared to the low-gradient River Mekong (0-60 cm/h) (Alin et al., 2011;Ran et al., 2015), due to higher flow velocity in the Yellow River (1.8 m/s) than Mekong river (0.9±0.4 m/s), resulting in greater surface turbulence and higher k_{600} level in the Yellow (42 ±17 cm/h) than Mekong river (15 ±9 cm/h). This could substantiate the higher k_{600} levels and spatial changes in k_{600} values of our three river systems. For instance, similar to other turbulent rivers in China (Ran et al., 2017;Ran et al., 2015), high k_{600} values in the TGR, Daning and Qjiang rivers were due to mountainous terrain catchment, high current velocity (10 – 150 cm/s) (Fig. 4b), bottom roughness, and shallow water depth (10 - 150 cm) (Fig. 4a). It has been suggested that shallow water enhances bottom shear, and the resultant turbulence increases k values (Alin et al., 2011;Raymond et al., 2012). These physical controls are highly variable across environmental types (Figs. 4a and 4b), hence, k values are expected to vary widely (Fig. 3). The k_{600} values in the TGR rivers showed wider range (1-177 cm/h; Fig. 3; Table S1), spanning more than 2 orders of magnitude across the region, and it is consistent with the considerable variability in the physical processes on water turbulence across environmental settings. Similar broad range of k_{600} levels was also observed in the China's Yellow basin (ca. 0-123 cm/h) (Ran et al., 2015;Ran et al., 2017).

Insignificant relationships between riverine k_{600} and wind speed were consistent with earlier studies (Alin et al., 2011;Raymond et al., 2012). The lack of strong correlation between k_{600} and physical factors using the combined data were probably due to combined effect of both flow velocity and water depth, as well as large diversity of channel morphology, both across and within river networks in the entire catchment (60, 000 km^2). This is further collaborated by weak correlations between k_{600} and flow velocity in the TGR rivers (Fig. 4), where one or two samples were taken for a large scale examination. We provided new insights into k_{600} parameterized using current velocity. Nonetheless, k_{600} from our flow velocity based model (Fig. 4b) was potentially largely overestimated with consideration of other measurements (Alin et al., 2015;Ran et al., 2015;Ran et al., 2017). When several extreme values were removed, k_{600} (cm/h) was parameterized as follows (k_{600} = 62.879FV + 6.8357, R^2= 0.52, p=0.019, FV-flow velocity with a unit of m/s), and this revised model was in good agreement with the model in the river networks of the Yellow River (Ran et al., 2017), but much lower than the model developed in the Yangtze system (Liu et al., 2017) (Fig. 4c). This was reasonable because of k_{600} values in the Yangtze system were from large rivers with higher turbulence than Yellow and our studied rivers. Furthermore, the determined k_{600} using FCs was, on average, consistent with the revised model (Table 2). These differences in relationship between spatial changes in k_{600} values and physical characteristics further corroborated heterogeneity of channel geomorphology and hydraulic conditions across the investigated rivers.

The subtropical streams and small rivers are biologically more active and are recognized to exert higher CO_2 areal flux to the atmosphere, however, their contribution to riverine carbon cycling is still poorly quantified because of data paucity and the absence of k in particular. Larger uncertainty of riverine CO_2 emission in China was anticipated by use of k_{600} from other continents or climate zones. For instance, k_{600} for CO_2 emission from tributaries in the Yellow River and karst rivers was originated from the model in the Mekong (Zhang et al., 2017), and Pearl (Yao et al., 2007), Longchuan (Li et al., 2012), and Metropolitan rivers (Wang et al., 2017), which are mostly from temperate regions. Our k_{600} values will therefore largely improve the estimation of CO_2 evasion from subtropical streams and small rivers, and improve to refine riverine carbon budget. More studies, however, are clearly needed to build the model, based on flow velocity and slope/water depth given the difficulty in k quantification on a large scale.

4.4. Implications for large scale estimation

We compared CO_2 areal flux by FCs and models developed here (Fig. 4) and other studies (Alin et al., 2011) (Tables 2 and 3). CO_2 evasion was estimated for rivers in China with k values ranged between 8 and 15 cm/h (Li et al., 2012;Yao et al., 2007;Wang et al., 2011) (Table S2). These estimates of CO_2 evasion rate were considerably lower than using present k_{600} values (48.4 ± 53.2 cm/h). For instance, CO_2 emission rates in the Longchuan River (e.g., k = 8 cm/h) and Pearl River tributaries (e.g., k = 8-15 cm/h) were 3 to 6 times higher using present k values compared to earlier estimates. We found that the determined k_{600} average was marginally beyond the levels from water depth based model and the model developed by Alin et al (Alin et al., 2011), while equivalent to the flow velocity based revised model, resulting in similar patterns of CO_2 emission rates (Table 2). Hence selection of k values would significantly hamper the accuracy of the flux estimation. Therefore k must be estimated along with pCO_2 measurements to accurate flux estimations.

We used our measured CO_2 emission rates by FCs for upscaling flux estimates during monsoonal period given the sampling in this period and it was found to be 0.70 Tg CO_2 (1 Tg=10^{12} g) for all rivers sampled in our study (Table 3a). The estimated emission in the monsoonal period was close to that of the revised model (0.71 $\pm$0.66 (95% confidence interval: 0.46 - 0.94) Tg CO_2), and using the determined k average, i.e., 0.69 $\pm$0.65 (95% confidence interval: 0.45-0.93) Tg CO_2, but slightly higher than the estimation using water-depth based model (0.54 $\pm$0.51 Tg CO_2) and Alin's model (0.53 $\pm$0.50 Tg CO_2) (Table 3b). This comparable CO_2 flux further substantiated the exclusion of extremely k_{600} values for developing model (Fig. 4). The CO_2 evasion comparison by variable approaches also implied that the original flow velocity based model (two extremely k_{600} values were included; Fig. 4b) largely over-estimated the CO_2 fluxes, i.e., 1.66 $\pm$1.55 (1.08-2.23) Tg CO_2, was 2.3-3 fold higher than other estimations (Table 3b), and our earlier evasion using TBL on the TGR river networks (Li et al., 2018). Moreover, our estimated CO_2 emission during monsoonal period also suggests that CO_2 annual emissions from rivers and streams in this area were previously underestimated, i.e., 0.03 Tg CO_2/y (Li et al., 2017) and 0.37-0.44 Tg CO_2/y (Yang et al., 2013) as the former used TBL model with a lower k level, and the latter employed floating chambers, but they both sampled very limited tributaries (i.e., 2-3 rivers). Therefore, measurements of k must be made mandatory along with pCO_2 measurement in the river and stream studies.

5. Conclusion

We provided first determination of gas transfer velocity (k) in the subtropical streams and small rivers in the upper Yangtze. High variability in k values (mean 48.4 ± 53.2 cm/h) was observed, reflecting the variability of morphological characteristics on water turbulence both within and across river networks. We highlighted that k estimate from empirical model should be pursued with caution and the significance of incorporating k measurements along with extensive pCO_2 investigation is highly essential for upscaling to watershed/regional scale carbon (C) budget.

Riverine pCO_2 and CO_2 areal flux showed pronounced spatial variability with much higher levels in the TGR rivers. The CO_2 areal flux was averaged at 133.1 ± 269.1 mmol/m^2/d using FCs, the resulting emission during monsoonal period was around 0.7 Tg CO_2, similar to the scaling up emission with the determined k, and the revised flow velocity based model, while marginally above the water depth based model. More work is clearly needed to refine the k modeling in the river systems of the upper Yangtze River for evaluating regional C budgets.

Acknowledgements

This study was funded by "the Hundred-Talent Program" of the Chinese Academy of Sciences (R53A362Z10; granted to Dr. Li), and the National Natural Science Foundation of China (Grant No. 31670473). We are grateful to Mrs. Maofei Ni and Tianyang Li, and Miss Jing Zhang for their assistance in the field works. Users can access the original data from an Appendix. Special thanks are given to editor David Butman and anonymous reviewers for improving the manuscript.

References

Abril, G., Bouillon, S., Darchambeau, F., Teodoru, C. R., Marwick, T. R., Tamooh, F., Omengo, F. O., Geeraert, N., Deirmendjian, L., Polsenaere, P., and Borges, A. V.: Technical Note: Large overestimation of pCO(2) calculated from pH and alkalinity in acidic, organic-rich freshwaters, Biogeosciences, 12, 67-78, 10.5194/bg-12-67-2015, 2015.

Alin, S. R., Rasera, M., Salimon, C. I., Richey, J. E., Holtgrieve, G. W., Krusche, A. V., and Snidvongs, A.: Physical controls on carbon dioxide transfer velocity and flux in low-gradient river systems and implications for regional carbon budgets, Journal of Geophysical Research-Biogeosciences, 116, 10.1029/2010jg001398, 2011.

Alin, S. R., Maria, D. F. F. L. R., Salimon, C. I., Richey, J. E., Holtgrieve, G. W., Krusche, A. V., and Snidvongs, A.: Physical controls on carbon dioxide transfer velocity and flux in low - gradient river systems and implications for regional carbon budgets, Journal of Geophysical Research Biogeosciences, 116, 248-255, 2015.

Alshboul, Z., and Lorke, A.: Carbon Dioxide Emissions from Reservoirs in the Lower Jordan Watershed, PLoS One, 10, e0143381, 10.1371/journal.pone.0143381, 2015.

Beaulieu, J. J., Shuster, W. D., and Rebholz, J. A.: Controls on gas transfer velocities in a large river, Journal of Geophysical Research-Biogeosciences, 117, 10.1029/2011jg001794, 2012.

Bodmer, P., Heinz, M., Pusch, M., Singer, G., and Premke, K.: Carbon dynamics and their link to dissolved organic matter quality across contrasting stream ecosystems, Science of the Total Environment, 553, 574-586, 10.1016/j.scitotenv.2016.02.095, 2016.

Borges, A. V., Delille, B., Schiettecatte, L. S., Gazeau, F., Abril, G., and Frankignoulle, M.: Gas transfer velocities of CO2 in three European estuaries (Randers Fjord, Scheldt, and Thames), Limnology and Oceanography, 49, 1630-1641, 2004.

Butman, D., and Raymond, P. A.: Significant efflux of carbon dioxide from streams and rivers in the United States, Nature Geoscience, 4, 839-842, 10.1038/ngeo1294, 2011.

Cole, J. J., and Caraco, N. F.: Carbon in catchments: connecting terrestrial carbon losses with aquatic metabolism, Marine and Freshwater Research, 52, 101-110, 10.1071/mf00084, 2001.

Cole, J. J., Prairie, Y. T., Caraco, N. F., McDowell, W. H., Tranvik, L. J., Striegl, R. G., Duarte, C. M., Kortelainen, P., Downing, J. A., Middelburg, J. J., and Melack, J.: Plumbing the Global Carbon Cycle: Integrating Inland Waters into the Terrestrial Carbon Budget, Ecosystems, 10, 172-185, 10.1007/s10021-006-9013-8, 2007.

Crusius, J., and Wanninkhof, R.: Gas transfer velocities measured at low wind speed over a lake, Limnology and Oceanography, 48, 1010-1017, 2003.

Erkkila, K.-M., Ojala, A., Bastviken, D., Biermann, T., Heiskanen, J. J., Lindroth, A., Peltola, O., Rantakari, M., Vesala, T., and Mammarella, I.: Methane and carbon dioxide fluxes over a lake: comparison between eddy covariance, floating chambers and boundary layer method, Biogeosciences, 15, 429-445, 10.5194/bg-15-429-2018, 2018.

Galfalk, M., Bastviken, D., Fredriksson, S. T., and Arneborg, L.: Determination of the piston velocity for water-air interfaces using flux chambers, acoustic Doppler velocimetry, and IR imaging of the water surface, Journal of Geophysical Research-Biogeosciences, 118, 770-782, 10.1002/jgrg.20064, 2013.

Golub, M., Desai, A. R., McKinley, G. A., Remucal, C. K., and Stanley, E. H.: Large Uncertainty in Estimating p

CO2

From Carbonate Equilibria in Lakes, Journal of Geophysical Research: Biogeosciences, 122, 2909-2924, 10.1002/2017jg003794, 2017.

Guerin, F., Abril, G., Serca, D., Delon, C., Richard, S., Delmas, R., Tremblay, A., and Varfalvy, L.: Gas transfer velocities of CO2 and CH4 in a tropical reservoir and its river downstream, Journal of Marine Systems, 66, 161-172, 10.1016/j.jmarsys.2006.03.019, 2007.

Hunt, C. W., Salisbury, J. E., and Vandemark, D.: Contribution of non-carbonate anions to total alkalinity and overestimation of <i>p</i>CO₂ in New England and New Brunswick rivers, Biogeosciences, 8, 3069-3076, 10.5194/bg-8-3069-2011, 2011.

Jean-Baptiste, P., and Poisson, A.: Gas transfer experiment on a lake (Kerguelen Islands) using He-3 and SF6, Journal of Geophysical Research-Oceans, 105, 1177-1186, 10.1029/1999jc900088, 2000.

Lauerwald, R., Laruelle, G. G., Hartmann, J., Ciais, P., and Regnier, P. A. G.: Spatial patterns in CO2 evasion from the global river network, Global Biogeochemical Cycles, 29, 534-554, 10.1002/2014gb004941, 2015.

Lewis, E., Wallace, D., and Allison, L. J.: Program developed for CO{sub 2} system calculations, ; Brookhaven National Lab., Dept. of Applied Science, Upton, NY (United States); Oak Ridge National Lab., Carbon Dioxide Information Analysis Center, TN (United States)ORNL/CDIAC-105; R&D Project: ERKP960; Other: ON: DE98054248; BR: KP 12 02; TRN: AHC29816%%16 United States 10.2172/639712 R&D Project: ERKP960; Other: ON: DE98054248; BR: KP 12 02; TRN: AHC29816%%16 OSTI as DE98054248 ORNL English, Medium: ED; Size: 40 p., 1998.

Li, S., Gu, S., Tan, X., and Zhang, Q.: Water quality in the upper Han River basin, China: The impacts of land use/land cover in riparian buffer zone, Journal of Hazardous Materials, 165, 317-324, 10.1016/j.jhazmat.2008.09.123, 2009.

Li, S., and Bush, R. T.: Revision of methane and carbon dioxide emissions from inland waters in India, Global Change Biology, 21, 6-8, 2015.

Li, S., Bush, R. T., Ward, N. J., Sullivan, L. A., and Dong, F.: Air-water CO2 outgassing in the Lower Lakes (Alexandrina and Albert, Australia) following a millennium drought, Science of the Total Environment, 542, 453-468, 10.1016/j.scitotenv.2015.10.070, 2016.

Li, S., Wang, F., Luo, W., Wang, Y., and Deng, B.: Carbon dioxide emissions from the Three Gorges Reservoir, China, Acta Geochimica, https://doi.org/10.1007/s11631-017-0154-6 10.1007/s11631-017-0154-6, 2017.

Li, S., Ni, M., Mao, R., and Bush, R. T.: Riverine CO2 supersaturation and outgassing in a subtropical monsoonal mountainous area (Three Gorges Reservoir Region) of China, Journal of Hydrology, 558, 460-469, https://doi.org/10.1016/j.jhydrol.2018.01.057, 2018.

Li, S. Y., Lu, X. X., He, M., Zhou, Y., Li, L., and Ziegler, A. D.: Daily CO2 partial pressure and CO2 outgassing in the upper Yangtze River basin: A case study of the Longchuan River, China, Journal of Hydrology, 466, 141-150, 10.1016/j.jhydrol.2012.08.011, 2012.

Li, S. Y., Lu, X. X., and Bush, R. T.: CO2 partial pressure and CO2 emission in the Lower Mekong River, Journal of Hydrology, 504, 40-56, 10.1016/j.jhydrol.2013.09.024, 2013.

Liu, S., Lu, X. X., Xia, X., Zhang, S., Ran, L., Yang, X., and Liu, T.: Dynamic biogeochemical controls on river pCO(2) and recent changes under aggravating river impoundment: An example of the subtropical Yangtze River, Global Biogeochemical Cycles, 30, 880-897, 10.1002/2016gb005388, 2016.

Liu, S., Lu, X. X., Xia, X., Yang, X., and Ran, L.: Hydrological and geomorphological control on CO2 outgassing from low-gradient large rivers: An example of the Yangtze River system, Journal of Hydrology, 550, 26-41, 10.1016/j.jhydrol.2017.04.044, 2017.

Lorke, A., Bodmer, P., Noss, C., Alshboul, Z., Koschorreck, M., Somlai-Haase, C., Bastviken, D., Flury, S., McGinnis, D. F., Maeck, A., Mueller, D., and Premke, K.: Technical note: drifting versus anchored flux chambers for measuring greenhouse gas emissions from running waters, Biogeosciences, 12, 7013-7024, 10.5194/bg-12-7013-2015, 2015.

Mao, R., Chen, H., and Li, S.: Phosphorus availability as a primary control of dissolved organic carbon biodegradation in the tributaries of the Yangtze River in the Three Gorges Reservoir Region, Science of the Total Environment, 574, 1472-1476, 10.1016/j.scitotenv.2016.08.132, 2017.

Martinsen, K. T., Kragh, T., and Sand-Jensen, K.: Technical note: A simple and cost-efficient automated floating chamber for continuous measurements of carbon dioxide gas flux on lakes, Biogeosciences, 15, 5565-5573, 10.5194/bg-15-5565-2018, 2018.

Podgrajsek, E., Sahlee, E., Bastviken, D., Holst, J., Lindroth, A., Tranvik, L., and Rutgersson, A.: Comparison of floating chamber and eddy covariance measurements of lake greenhouse gas fluxes, Biogeosciences, 11, 4225-4233, 10.5194/bg-11-4225-2014, 2014.

Prytherch, J., Brooks, I. M., Crill, P. M., Thornton, B. F., Salisbury, D. J., Tjernstrom, M., Anderson, L. G., Geibel, M. C., and Humborg, C.: Direct determination of the air-sea CO2 gas transfer velocity in Arctic sea ice regions, Geophysical Research Letters, 44, 3770-3778, 10.1002/2017gl073593, 2017.

Ran, L., Li, L., Tian, M., Yang, X., Yu, R., Zhao, J., Wang, L., and Lu, X. X.: Riverine CO2 emissions in the Wuding River catchment on the Loess Plateau: Environmental controls and dam impoundment impact, Journal of Geophysical Research-Biogeosciences, 122, 1439-1455, 10.1002/2016jg003713, 2017.

Ran, L. S., Lu, X. X., Yang, H., Li, L. Y., Yu, R. H., Sun, H. G., and Han, J. T.: CO2 outgassing from the Yellow River network and its implications for riverine carbon cycle, Journal of Geophysical Research-Biogeosciences, 120, 1334-1347, 10.1002/2015jg002982, 2015.

Raymond, P. A., and Cole, J. J.: Gas exchange in rivers and estuaries: Choosing a gas transfer velocity, Estuaries, 24, 312-317, 10.2307/1352954, 2001.

Raymond, P. A., Zappa, C. J., Butman, D., Bott, T. L., Potter, J., Mulholland, P., Laursen, A. E., Mcdowell, W. H., and Newbold, D.: Scaling the gas transfer velocity and hydraulic geometry in streams and small rivers, Limnology & Oceanography Fluids & Environments, 2, 41–53, 2012.

Raymond, P. A., Hartmann, J., Lauerwald, R., Sobek, S., McDonald, C., Hoover, M., Butman, D., Striegl, R., Mayorga, E., Humborg, C., Kortelainen, P., Duerr, H., Meybeck, M., Ciais, P., and Guth, P.: Global carbon dioxide emissions from inland waters, Nature, 503, 355-359, 10.1038/nature12760, 2013.

Schilder, J., Bastviken, D., van Hardenbroek, M., Kankaala, P., Rinta, P., Stötter, T., and Heiri, O.: Spatial heterogeneity and lake morphology affect diffusive greenhouse gas emission estimates of lakes, Geophysical Research Letters, 40, 5752-5756, 10.1002/2013gl057669, 2013.

Tranvik, L. J., Downing, J. A., Cotner, J. B., Loiselle, S. A., Striegl, R. G., Ballatore, T. J., Dillon, P., Finlay, K., Fortino, K., and Knoll, L. B.: Lakes and reservoirs as regulators of carbon cycling and climate, Limnology & Oceanography, 54, 2298-2314, 2009.

Wang, F., Wang, B., Liu, C. Q., Wang, Y., Guan, J., Liu, X., and Yu, Y.: Carbon dioxide emission from surface water in cascade reservoirs–river system on the Maotiao River, southwest of China, Atmospheric Environment, 45, 3827-3834, 2011.

Wang, X. F., He, Y. X., Yuan, X. Z., Chen, H., Peng, C. H., Zhu, Q., Yue, J. S., Ren, H. Q., Deng, W., and Liu, H.: pCO(2) and CO2 fluxes of the metropolitan river network in relation to the urbanization of Chongqing, China, Journal of Geophysical Research-Biogeosciences, 122, 470-486, 10.1002/2016jg003494, 2017.

Wanninkhof, R.: RELATIONSHIP BETWEEN WIND-SPEED AND GAS-EXCHANGE OVER THE OCEAN,

Journal of Geophysical Research-Oceans, 97, 7373-7382, 10.1029/92jc00188, 1992.
Wanninkhof, R., and Knox, M.: Chemical enhancement of CO2 exchange in natural waters, Limnology and Oceanography, 41, 689-697, 10.4319/lo.1996.41.4.0689, 1996.
Wanninkhof, R., Asher, W. E., Ho, D. T., Sweeney, C., and McGillis, W. R.: Advances in Quantifying Air-Sea Gas Exchange and Environmental Forcing, Annual Review of Marine Science, 1, 213-244, 10.1146/annurev.marine.010908.163742, 2009.
Xiao, S., Yang, H., Liu, D., Zhang, C., Lei, D., Wang, Y., Peng, F., Li, Y., Wang, C., Li, X., Wu, G., and Liu, L.: Gas transfer velocities of methane and carbon dioxide in a subtropical shallow pond, Tellus Series B-Chemical and Physical Meteorology, 66, 10.3402/tellusb.v66.23795, 2014.
Yang, L., Lu, F., Wang, X., Duan, X., Tong, L., Ouyang, Z., and Li, H.: Spatial and seasonal variability of CO2 flux at the air-water interface of the Three Gorges Reservoir, Journal of Environmental Sciences, 25, 2229-2238, https://doi.org/10.1016/S1001-0742(12)60291-5, 2013.
Yao, G. R., Gao, Q. Z., Wang, Z. G., Huang, X. K., He, T., Zhang, Y. L., Jiao, S. L., and Ding, J.: Dynamics Of CO2 partial pressure and CO2 outgassing in the lower reaches of the Xijiang River, a subtropical monsoon river in China, Science of the Total Environment, 376, 255-266, 10.1016/j.scitotenv.2007.01.080, 2007.
Zhang, J., Li, S., Dong, R., and Jiang, C.: Physical evolution of the Three Gorges Reservoir using advanced SVM on Landsat images and SRTM DEM data, Environmental Science and Pollution Research, 25, 14911-14918, 10.1007/s11356-018-1696-9, 2018.
Zhang, T., Li, J., Pu, J., Martin, J. B., Khadka, M. B., Wu, F., Li, L., Jiang, F., Huang, S., and Yuan, D.: River sequesters atmospheric carbon and limits the CO2 degassing in karst area, southwest China, Science of The Total Environment, 609, 92-101, https://doi.org/10.1016/j.scitotenv.2017.07.143, 2017.

Table 1. Statistics of all the data from three river systems (separated statistics please refer to Figs. S2 and S3 in the Supplementary material).

		Water T (^{0}C)	pH	Alkalinity (μeq/l)	pCO$_2$ (μatm)	DO%	DOC (mg/L)
Number		115	115	115	115	56	114
Mean		22.5	8.39	2589.1	846.4	91.5	6.67
Median		22.8	8.46	2560	588.4	88.8	2.51
Std. Deviation		6.3	0.29	640.7	818.5	8.7	7.62
Minimum		11.7	7.47	600	50.1	79.9	0.33
Maximum		34	9.38	4488	4830.4	115.9	37.48
Percentiles	25	16.3	8.24	2240	389.8	84.0	1.33
	75	29	8.56	2920	920.4	99.1	9.96
95% CI for Mean	Lower Bound	21.4	8.33	2470.8	695.2	89.1	5.26
	Upper Bound	23.7	8.44	2707.5	997.6	93.8	8.09

CI-Confidence Interval.

Table 2. Comparison of different model for CO_2 areal flux estimation using combined data (unit is mmol/m^2/d for CO_2 areal flux and cm/h for k_{600}).

		From FC	Flow velocity-based model (Fig. 4b)[a]	Water depth-based model (Fig.3a)	Alin's model
k_{600}		48.4[b]	116.5[c]	38.3	37.6
CO_2 areal flux					
Mean		198.1	476.7	156.6	154.0
S.D.		185.5	446.2	146.6	144.2
95% CI for Mean[a]	Lower Bound	129.5	311.5	102.3	100.6
	Upper Bound	266.8	641.8	210.8	207.4

CI-Confidence Interval

[a]Flow velocity –based model is from a subset of the data (please refer to Fig. 4)

[b]Mean value determined using floating chambers (FC).

c-This figure is revised to be 49.6 cm/h if the model (k_{600} = 62.879FV + 6.8357, R^2= 0.52, p=0.019) is used (the model is obtained by taking out two extremely values; please refer to Fig. 4c), and the corresponding CO_2 areal flux is 203±190 mmol/m^2/d.

Table 3. CO_2 emission during monsoonal period (May through Oct.) from total rivers sampled in the study.

(a) Upscaling using CO_2 areal flux (mean ± S.D.) by FC during monsoonal period.

	Catchment Area km^2	Water surface km^2	CO_2 areal flux $mmol/m^2/d$	CO_2 emission Tg CO_2
Daning	4200	21.42	122.0 ± 239.4	0.021
Qijiang	4400	30.8	50.3 ± 177.2	0.0125
TGR river	50000	377.78	217.7 ± 334.7	0.666
Total				0.70

(b) Upscaling using determined k_{600} average and models (whole dataset are used here).

		From determined k_{600} mean	Flow velocity-based model (Fig. 4b) (numbers in bracket is from the revised model; Fig. 4c)	Water depth-based model (Fig. 4a)	Alin's model
Mean		0.69	1.66 (0.71)	0.54	0.53
S.D.		0.65	1.55 (0.66)	0.51	0.50
95% CI for Mean	Lower Bound	0.45	1.08 (0.46)	0.36	0.35
	Upper Bound	0.93	2.23 (0.94)	0.74	0.72

A total water area of approx. 430 km^2 for all tributaries (water area is from Landsat ETM+ in 2015); CO_2 emission upscaling (Tg CO_2 during May through October) was conducted during the monsoonal period because of the sampling in this period.

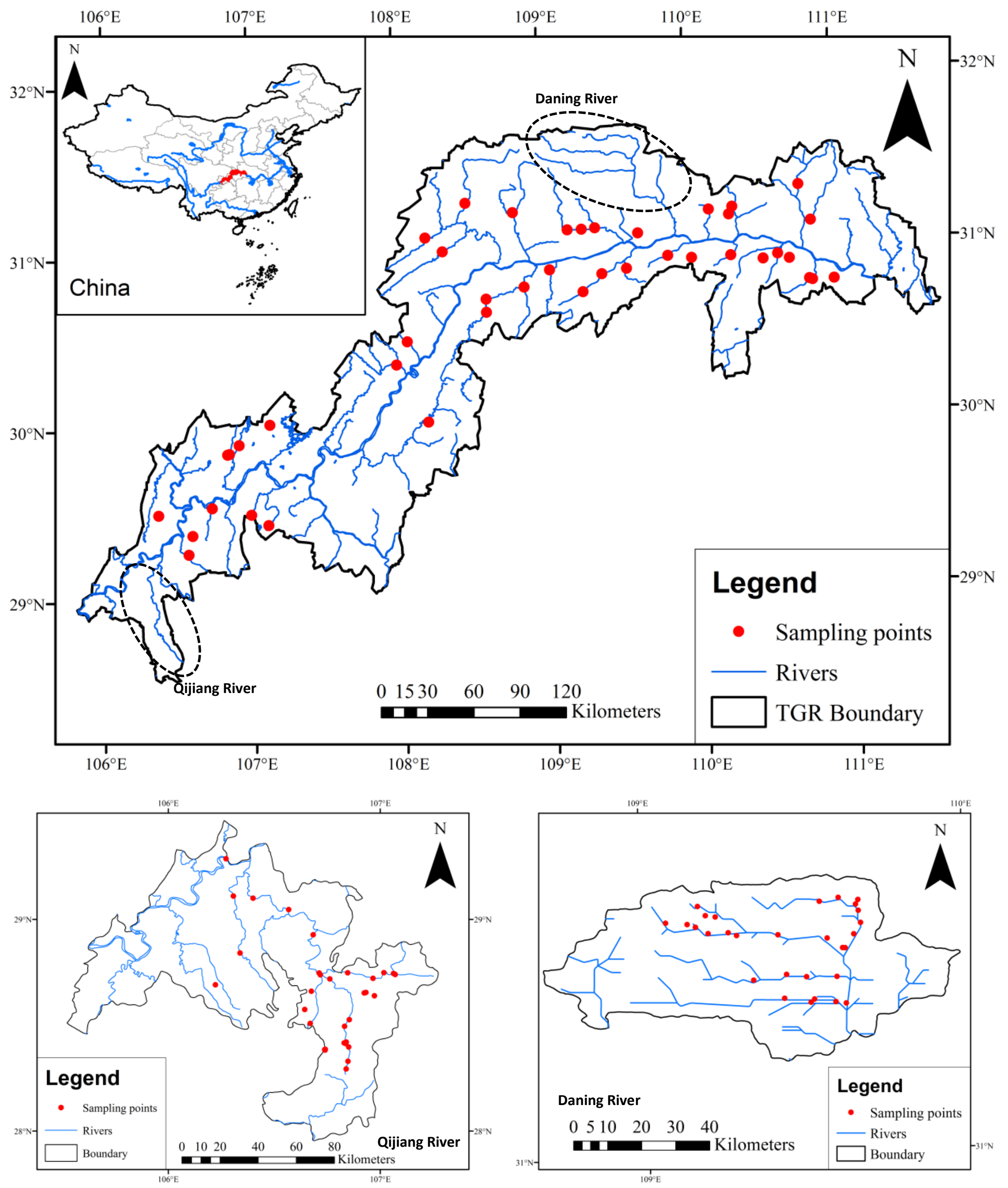

Fig. 1. Map of sampling locations of major rivers and streams in the Three Gorges Reservoir region, China.

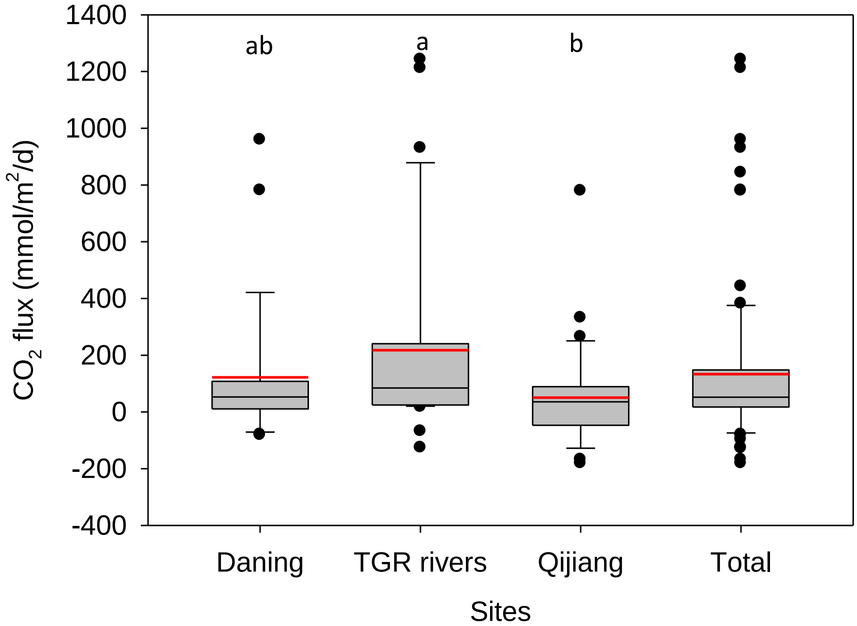

Fig. 2. Boxplots of CO_2 emission rates by floating chambers in the investigated three river systems (different letters represent statistical differences at $p<0.05$ by Mann-Whitney Rank Sum Test). (the black and red lines, lower and upper edges, bars and dots in or outside the boxes demonstrate median and mean values, 25th and 75th, 5th and 95th, and <5th and >95th percentiles of all data, respectively). (For interpretation of the references to color in this figure legend, the reader is referred to the web version of this article) (Total means combined data from three river systems).

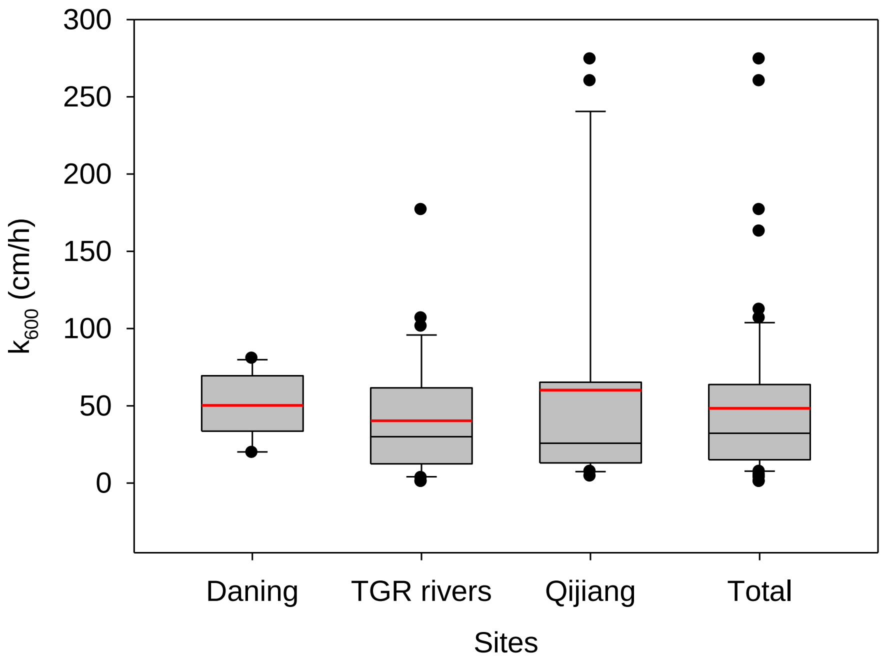

Fig. 3. Boxplots of k_{600} levels in the investigated three river systems (there is not a statistically significant difference in k among sites by Mann-Whitney Rank Sum Test). (the black and red lines, lower and upper edges, bars and dots in or outside the boxes demonstrate median and mean values, 25th and 75th, 5th and 95th, and <5th and >95th percentiles of all data, respectively). (For interpretation of the references to color in this figure legend, the reader is referred to the web version of this article) (Total means combined data from three river systems).

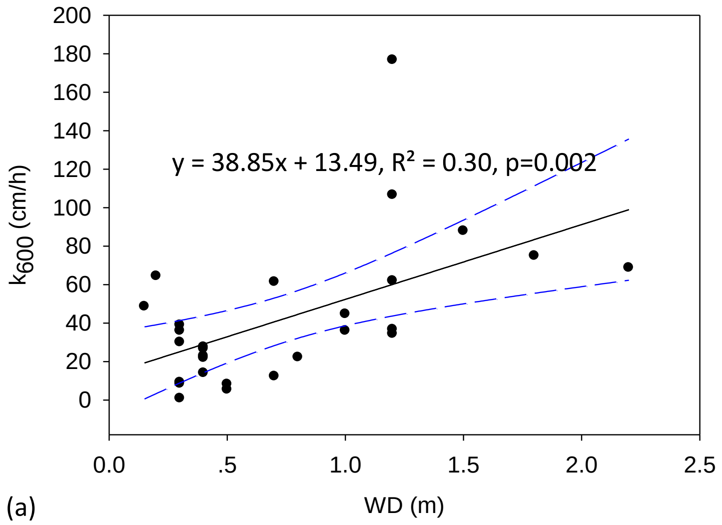

(a)

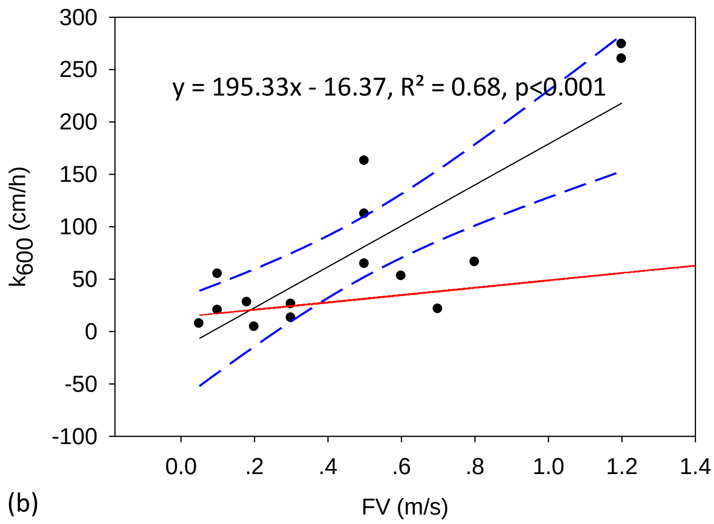

(b)

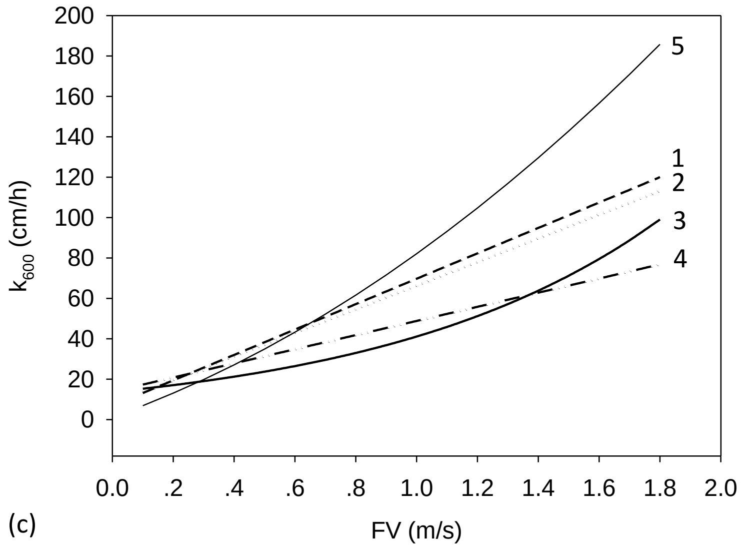

(c)

Fig. 4. The k_{600} as a function of water depth (WD) using data from TGR rivers (a), flow velocity (FV) using data from Qijiang (b), and comparison of the developed model

with other models (c) (others without significant relationships between k and physical factors are not shown). The solid lines show regression, the dashed lines represent 95% confidence band, and the red dash-dotted line represents the model developed by Alin et al (2011) (Extremely values of 260 and 274 cm/h are removed in panel b, the revised model would be k_{600} = 62.879FV + 6.8357, R^2 = 0.52, p=0.019) (in panel c, 1-the revised model, 2-model from Ran et al., 2017, 3-model from Ran et al., 2015, 4-model from Alin et al,, 2011, 5-model from Liu et al., 2017) (1- k_{600} = 62.879FV + 6.8357; 2- k_{600} = 58.47FV+7.99; 3- k_{600} = 13.677exp (1.1FV); 4- k_{600} = 35 FV + 13.82; 5- k_{600} = $6.5FV^2$ + 12.9FV+0.3) (unit of k in models 1-4 is cm/h, and unit of m/d for model 5 is transferred to cm/h).